Bull. Mater. Sci., Vol. 39, No. 1, February 2016, pp. 331–336. © Indian Academy of Sciences.

Preparation of new thermoluminescent material $(100-x)B_2O_3$–xLi_2O: Cu^{2+} for sensing and detection of radiation

ZEID A ALOTHMAN, TANSIR AHAMAD, MU NAUSHAD* and SAAD M ALSHEHRI
Department of Chemistry, College of Science, Bld #5, King Saud University, Riyadh 11451, Saudi Arabia

MS received 15 April 2015; accepted 7 September 2015

Abstract. The copper-doped lithium borate glass as a thermoluminescent (TL) material $(100-x)B_2O_3$–$xLi_2O : Cu^{2+}$ ($x = 20$, 50 and 80 mol%) was prepared by the combustion method. The formation of $(100-x)B_2O_3$–$xLi_2O : Cu^{2+}$ after doping 2, 3 and 5 ppm Cu^{2+}, was characterized by Fourier transform infrared spectroscopy, X-ray diffraction and transmission electron microscopy. The TL characteristics of the synthesized material were studied at different parameters. The synthesized glass $50B_2O_3$–$50i_2O : Cu^{2+}$ with 3 ppm of doped Cu^{2+}, exhibited the superior TL properties than other glasses prepared in the current study. The spin-Hamiltonian parameters were assessed using the electron spin resonance spectra of $50B_2O_3$–$50Li_2O : Cu^{2+}$ doped with 3 ppm Cu^{2+}. The spin-Hamiltonian parameter values in the case of Cu^{2+} revealed that the ground state of Cu^{2+} was dx^2-y^2 orbital ($^2B_{1g}$) and the site symmetry around Cu^{2+} ion was distorted octahedral. TL glow curves were recorded with different heating rates (1, 2, 5, 10, 15, and 20°C s^{-1}) at the fixed dose 10×10^3 Gy. The results revealed that the glow peak position shifted to higher temperature with heating rate and the heating rate of 10°C s^{-1} showed the superior TL response with highest glow peak which is very good for dosimetry purposes.

Keywords. Inorganic compounds; glasses; nanostructures; transmission electron microscopy; luminescence.

1. Introduction

Thermally stimulated luminescence or thermoluminescence (TL) is thermally stimulated emission of the irradiation-induced electrons from a semiconductor or insulator after absorption of energy from radiation such as X-rays, gamma rays, high-energy electron beam, etc. [1,2]. The TL results can provide several appreciated information regarding the materials such as the intrinsic defects and the energetic ray to which the material was subjected. Therefore, it is extensively used in the field of irradiation detection, defect studying and archaeology dating [3–5]. From last four decade, much effort has been tried to find new and high-performance TL materials with the increasing demand of this field and used in the environment, personal and clinical ionizing radiation protection. Several materials, e.g., sulphate, fluoride, phosphate, borate and oxide have been explored as thermoluminescence dosimetry (TLD) materials [6–14]. ZnS, $Sr_2Mg(BO_3)_2$, MgB_4O_7 and $CaSO_4$ with different dopants have been extensively studied in the luminescence dosimetry but their suitability for temperature sensing applications has not been explored [15,16]. On the other hand, mechanical strength, low melting temperature, chemical stability, capability to accommodate various transition metal ions and other favourable properties has made lithium borate glass a potential TLD. Because of the high sensitivity and tissue equivalence, borate is one type of material appropriate for personal dosimetry and many research works on borate TL materials have been carried out because of its effective atomic number very close to human tissue ($Z_{eff} = 7.42$) [17–22]. The metal ions-doped lithium borate dosimeter may lead to a pure form. Several metal-doped lithium borates have been proposed as a thermoluminescent material. This dosimeter had low TL sensitivity due to its high wavelength emission (600 nm) as compared to the photomultiplier tube (PMT) (400–500 nm). A promising sensitivity was attained by activating the lithium borate with copper ions. Several studies disclosed that copper is one of the most effective activators. Many investigators have studied dosimetric properties of borate glasses activated with copper ions or co-activated with copper and other metal ions [23,24]. The present research was focused on the new borate glasses modified with lithium and potassium carbonate and co-doped with various metals Cu^{2+}. The structural and morphological characterizations of prepared samples were carried out using X-ray diffraction (XRD). The TL glow curve exhibited two peaks centred at around 105 and 210°C.

2. Experimental

2.1 *Preparation of $(100-x)B_2O_3$–$xLi_2O : Cu^{2+}$*

The well-known solid-state reaction method was used to prepare $(100-x)B_2O_3$–$xLi_2O : Cu^{2+}$. The raw materials such as Li_2CO_3 (99.998%, Sigma-Aldrich), H_3BO_3 (99.99%,

*Author for correspondence (shad81@rediffmail.com)

Sigma-Aldrich) and $CuNO_3$ (99.99%, Sigma-Aldrich) are used as received. Powders are weighed according to the formula: B_2O_3–xLi_2O : Cu^{2+}, where $x = 20$, 50 and 80 with 2, 3 and 5 ppm of $Cu(NO_3)_3{\cdot}6H_2O$ was used as a doping agent. The polycrystalline powder was put in ultraclean plastic bottles along with ceramic balls and ball milled for several hours. The well-mixed powder was shifted to an argon-purged glove box and loaded into alumina crucible. For sintering, the alumina crucible was slowly heated in a furnace at the rate of 100°C h^{-1} in order to achieve 725°C temperature. The powder was kept at 725°C for 25 h and after that it was cooled down to room temperature at the same rate of 100°C h^{-1}. Then the sintered powder was grinded in agate mortar. The whole process of ball milling, heating and grinding was repeated twice in order to sinter the powder well.

2.2 *Characterization*

The infrared spectra of the $(100-x)B_2O_3$–xLi_2O and $(100-x)B_2O_3$–xLi_2O : Cu^+ were recorded using ATR–FTIR spectra from 4000 to 600 cm^{-1} using a Bruker Tensor 27 instrument equipped with a MCT detector as the average of 32 scans at 2 cm^{-1} resolution. The system was managed by Bruker OPUS software. To confirm the formation of $(100-x)B_2O_3$–xLi_2O : Cu^{2+}, XRD pattern were taken at room temperature using X'pert Pro X-ray diffractometer (PANalytical) with Cu Kα radiation. The mean coherence lengths (MCL) perpendicular to some crystallographic planes of the $(100-x)B_2O_3$–xLi_2O : Cu^{2+} samples were calculated from strong reflections with percentage intensity by measuring the full-width at half-maximum (FWHM). To calculate the particle size, the Debye–Scherrer equation is given as

$$D = \frac{K\lambda}{\beta \cos\theta},$$

where λ is the wavelength of light used for the diffraction, K the Scherrer constant, β the 'full-width at half-maximum' of the sharp peaks, and θ the angle measured. The shape and particle of the concerned phosphor were also analysed by transmission electron microscopy (FE-TEM, JEM-2100F, JEOL). For the TEM characterizations, a drop of the sample in the form of colloidal suspension was deposited onto a lacey-carbon copper grid. The elements present in the samples were determined by chemical analyses through energy-dispersive spectrometry analyzer (EDS) integrated in the transmission electron microscope. To study the TL properties, the samples were exposed to γ-rays using ^{60}Co source for different doses (1×10^{-3} to 20×10^3 Gy). TL glow curves were recorded by Harshaw TLD reader (Model 3500) fitted with a 931B photomultiplier (PMT). The heating rate was 1, 2, 5, 10, 15 and 20°C s^{-1}. The equal quantity of sample (5 mg) was taken each time for recording TL.

3. Results and discussion

The structure of binary lithium borate glasses $(100-x)B_2O_3$–xLi_2O consists of random network of BO_3 triangles with certain fraction of boroxol rings. In the case of $50B_2O_3$–$50Li_2O$ spectra as given in figure 1a, a weak band appeared around 411 cm^{-1} showing the presence of lithium oxide in the glass samples [11]. Another band appeared around 435 cm^{-1} which could be due to the vibration of lithium cations [12]. The band at 475–508 cm^{-1} could be due to B–O–B bonds bending vibrations. The band around 621 cm^{-1} might be due to some deformation modes of the network structure. Two major bands around 968 and 1449 cm^{-1} ascribed to the B–O bond stretching of BO_4 and diborate groups. The bands between 1200 and 1605 cm^{-1} were due to the asymmetric stretching relaxation of B–O bond of trigonal BO_3 units of system $(100-x)B_2O_3$–xLi_2O. The band in the region 3200–3600 cm^{-1} was due to hydroxyl or water groups present in the glass. It was observed that the Cu^{2+}-doped lithium borate glasses $50B_2O_3$–$50Li_2O$: Cu^{2+} doped with 3 ppm Cu^{2+} showed all the peaks similar to that of corresponding un-doped glass as shown in figure 1b, but some additional bands were observed at 527 and 464 cm^{-1} which were due to the Cu–O and Cu^{2+} ions, respectively.

The optical absorption spectra of $50B_2O_3$–$50Li_2O$ and $50B_2O_3$–$50Li_2O$: Cu^{2+} doped with 3 ppm Cu^{2+} is given in figure 2. Absorption spectrum of $50B_2O_3$–$50Li_2O$ glass exhibited good transparency with its absorption in UV region (UV-transmission ability). A single absorption band in the near-infrared region was observed for $50B_2O_3$–$50Li_2O$: Cu^{2+}. This band was in the near-infrared region can be identified as d–d transition band due to Cu^{2+} ions and could be described in terms of ligand field theory [25,26]. In glasses, it is expected that due to vitreous state disorder, no site is perfectly cubic. Therefore, tetragonal distortions are endemic to the vitreous state which leads to the splitting of energy levels. It is observed that the elongated structures are usually more energetically favoured than the compressed ones [27]. Hence, in the present study, the observed asymmetric band was due to the overlap of $^2B_{1g} \rightarrow {}^2A_{1g}$ and $^2B_{1g} \rightarrow {}^2B_{2g}$ transitions.

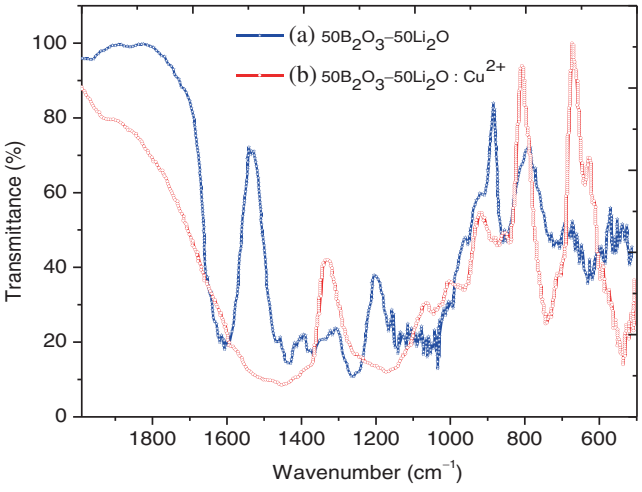

Figure 1. FTIR spectra (**a**) $50B_2O_3$–$50Li_2O$ and (**b**) $50B_2O_3$–$50Li_2O$: Cu^{2+} doped with 3 ppm Cu^{2+}.

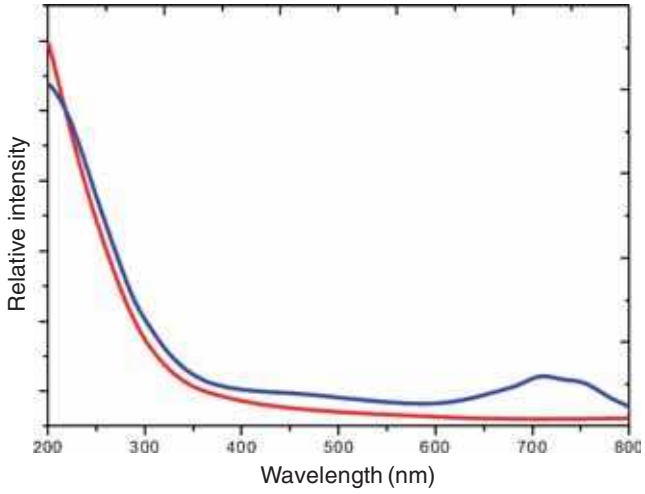

Figure 2. UV–visible spectra of $50B_2O_3$–$50Li_2O$: Cu^{2+} doped with 3 ppm Cu^{2+}.

The Cu^{2+} ions, with effective spin $S = 1/2$, has a nuclear spin $I = 3/2$ show various parallel and perpendicular hyperfine structures. In the electron spin resonance (ESR) spectrum of $50B_2O_3$–$50Li_2O$: Cu^{2+} doped with 3 ppm Cu^{2+}, four weak parallel hyperfine structure were observed in the lower magnetic field region and fourth parallel hyperfine structure were overlapped with the perpendicular hyperfine structure. The perpendicular hyperfine structure in the high magnetic field region was not resolved. It was observed that high magnetic field region of the spectra was more intense than the low magnetic field region and supported by reported data for other TL glass systems [28–31]. An axial spin-Hamiltonian was employed in the analysis of EPR spectra [31,32], which is given as

$$H = \beta\left[g_{||}H_Z S_Z + g_{\perp}\left(S_X H_X + S_Y H_Y\right) + A_{||}I_Z S_Z + A_{\perp}\left(S_X I_X + S_Y I_Y\right)\right],$$

where $g_{||}$ and $g_{\perp}$ the parallel and perpendicular hyperfine structures of tensor g and $A_{||}$ and $A_{\perp}$ are parallel and perpendicular hyperfine structures of tensor A. β is the Bohr magneton, S and I are the electron and nuclear spin operators, H_X, H_Y and H_Z the static magnetic field components. X and Y are the axis while Z is the symmetry axis.

The nuclear quadrupole contribution is neglected [33]. The solution to the spin-Hamiltonian gives the following expressions for the peak position related to the principal values of g and A tensors [34], for the parallel and perpendicular hyperfine peaks, respectively:

$$h\upsilon = g_{\perp}\beta H + mA_{\perp} + \left(\frac{15}{4} - m^2\right)\frac{A_{\perp}^2 + A_{||}^2}{4g_{\perp}\beta H}$$

and

$$h\upsilon = g_{||}\beta H + mA_{||} + \left(\frac{15}{4} - m^2\right)\frac{A_{\perp}^2}{2g_{||}\beta H},$$

where m is the nuclear magnetic quantum number of the copper nucleus with the values $+3/2$, $+1/2$ $-1/2$ and $-3/2$, and $\upsilon$is the microwave frequency. The spin-Hamiltonian parameters have been found to be 135.20×10^4 and 26.48×10^4 for $A_{||}$ and $A_{\perp}$, respectively.

It was observed that, $g^{\mathrm{II}} > g^{\perp}$ with these values $g^{\mathrm{II}} = 2.348$, $g^{\perp} = 2.114$ as shown in figure 3. These values indicated that the ground state of Cu^{2+} revealed that the ground state of Cu^{2+} was dx^2–y^2 orbital ($^2B_{1g}$) and the site symmetry around Cu^{2+} ion was distorted octahedral [8]. It was also observed that the obtained absorption spectra were asymmetric, characteristic of Cu^{2+} ($3d^9$) ions in axially distorted octahedral symmetric sites [35,36]. It was found that the spectra kept their overall aspect in the entire composition range suggested high structural stability of the glassy matrix to accept Cu^{2+} ions. The covalent character of a bond becomes more pronounced when the parameters g^{II} and $g^{\perp}$ were decreased. The most sensitive parameter is the g^{II}, the variation in the g^{II} value is the best indication about the covalent character. According to Kivelson and Neimen, for ionic environment the g^{II} value is normally >2.3 and for the covalent character the value is <2.3. The g-values can be used to calculate the G-value, with this factor indicating that the ligand is a weak field or strong field ligand. The equation used is as follows:

$$G = \left(g^{\mathrm{II}} - 2.002\right)/(g^{\perp} - 2.002),$$

where G is less than 4.0, the ligand forming Cu^{2+} complex is regarded as a strong field ligand. In this case, the G-value is 3.08, which indicated the formation of a strong field ligand [37,38].

The formation of synthesized compound was confirmed by studying the XRD pattern which is shown in figure 4. Using the XRD pattern, the average particle size of $50B_2O_3$–$50Li_2O$: Cu^{2+} doped with 3 ppm Cu^{2+} was calculated to be approximately 54 nm. The shape and the size of the particles of the $50B_2O_3$–$50Li_2O$: Cu^{2+} doped with 3 ppm Cu^{2+}

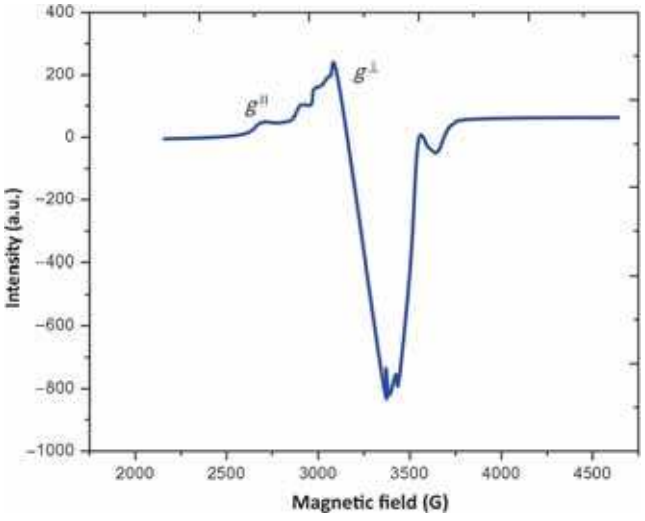

Figure 3. ESR spectral of $50B_2O_3$–$50Li_2O$: Cu^{2+} doped with 3 ppm Cu^{2+}.

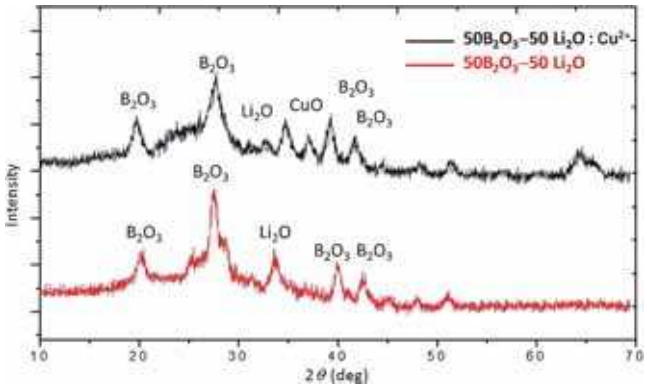

Figure 4. XRD patterns of $50B_2O_3$–$50Li_2O$ and $50B_2O_3$–$50Li_2O$: Cu^{2+} doped with 3 ppm Cu^{2+}.

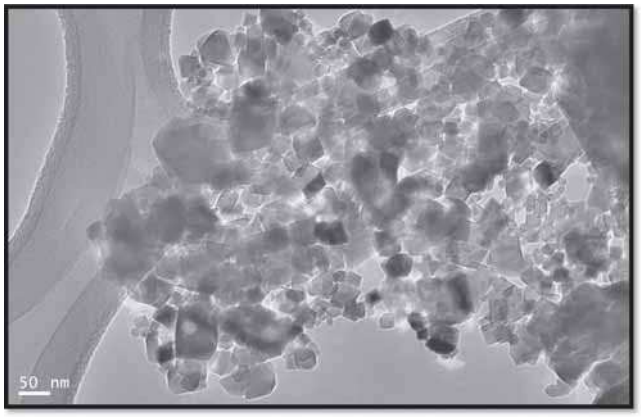

Figure 5. TEM image of $50B_2O_3$–$50Li_2O$: Cu^{2+} doped with 3 ppm Cu^{2+}.

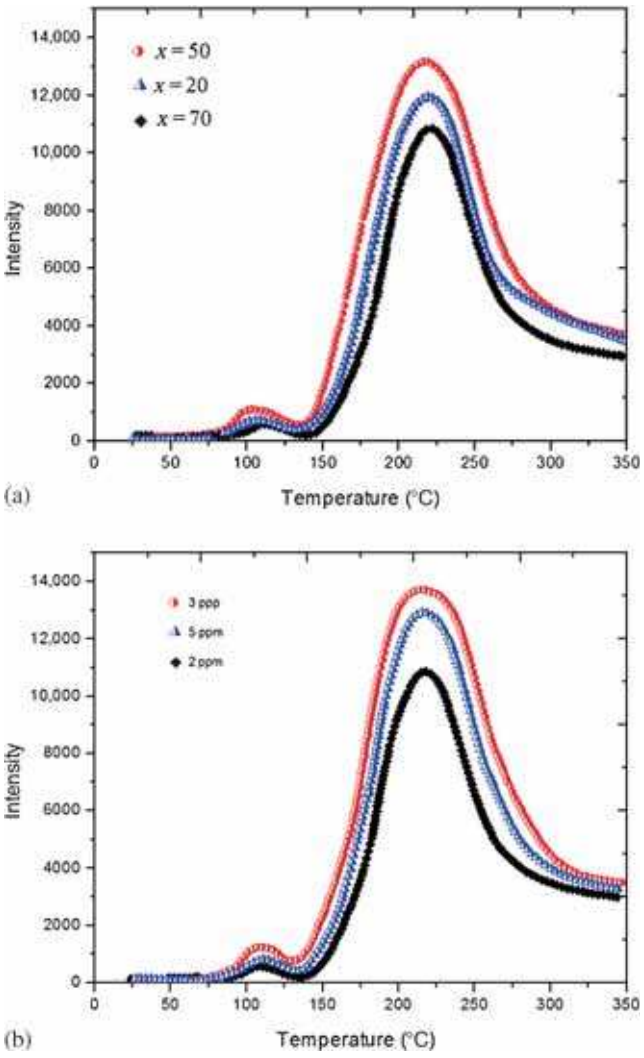

Figure 6. (**a**) TL glow curves of glass doped with 3 ppm for $20B_2O_3$–$80Li_2O$: Cu^{2+}, $50B_2O_3$–$50Li_2O$: Cu^{2+} and $70B_2O_3$–$30Li_2O$: Cu^{2+}. (**b**) TL glow curves of $50B_2O_3$–$50Li_2O$: Cu^{2+} glass doped with 2, 3 and 5 ppm Cu^{2+}.

were also evaluated by transmission electron microscopy (TEM). The TEM photograph showed that the particles were of cubic shape with their average length was in the range of approximately 30–80 nm as shown in figure 5.

The TL properties of synthesized copper-doped lithium borate glasses was performed with three different concentrations of Li_2O (30, 50 and 80 mol%). The selected glass ($50B_2O_3$–$50Li_2O$) containing 50 mol% of Li_2O was further doped with 2, 3 and 5 ppm of Cu^{2+}.

The TL intensity as a function of temperature for $(100-x)B_2O_3$–xLi_2O : Cu^{2+} (x = 30, 50 and 80) doped with 3 ppm of Cu^{2+} exposed to a gamma dose of 10×10^3 Gy from the ^{60}Co source are illustrated in figure 6. The TL glow curve of this glass sample had a weak peak with very low intensity at 102°C and other prominent at very high intensity around 225°C. It was observed that $50B_2O_3$–$50Li_2O$: Cu^{2+} showed the highest TL intensity than $70B_2O_3$–$30Li_2O$: Cu^{2+} and $20B_2O_3$–$80Li_2O$: Cu^{2+}, while $20B_2O_3$–$80Li_2O$: Cu^{2+} showed higher TL intensity than that of $70B_2O_3$–$30Li_2O$: Cu^{2+} as shown in figure 6a. The effect of the doping agent concentration on TL glow curves were carried out using $50B_2O_3$–$50Li_2O$ with the doping 2, 3 and 5 ppm of Cu^{2+} and illustrated in figure 6b. When these samples were exposed to a gamma dose of 10×10^3 Gy from the ^{60}Co source, it was found that the glass doped with 3 ppm Cu^{2+} showed the superior TL intensity (13,752 μC, micro-Coulomb) than that of 5 and 2 ppm Cu^{2+}. The effect of gamma dose on TL glow curves of synthesized $50B_2O_3$–$50Li_2O$: Cu^{2+} doped with 3 ppm were recorded and the glow curves are shown in figure 7a. It was noted that with the increase in dose from 0.5×10^3 to 20×10^3 Gy, the TL intensity was increased and the prominent glow peaks appeared between 200 and 250°C. To see the effect of the heating rate on the TL intensity, the experiments were carried out using $50B_2O_3$–$50Li_2O$: Cu^{2+} doped with 3 ppm exposed to a fix gamma dose of 10×10^3 Gy and the results are illustrated in figure 7b. The result revealed that the heating rate changed both the intensity and peak position of the glow curves. It was also observed that the heating rate of 10°C s^{-1} was most suitable heating rate to obtained superior TL intensity and suitable glow peak temperature. The role of Cu^{2+} in $50B_2O_3$–$50Li_2O$ was to create

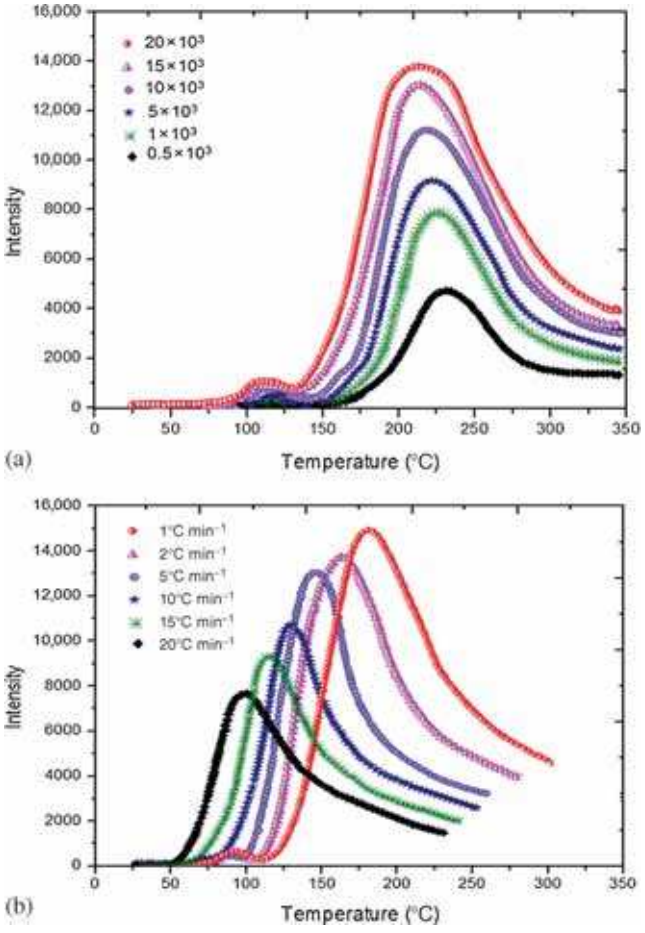

Figure 7. TL glow curves of $50B_2O_3$–$50Li_2O$: Cu^{2+} doped with 3 ppm (**a**) at different gamma doses between 0.5×10^3 and 20×10^3 Gy and (**b**) at different heating rates namely 1, 2, 5, 10, 15 and 20°C s^{-1}.

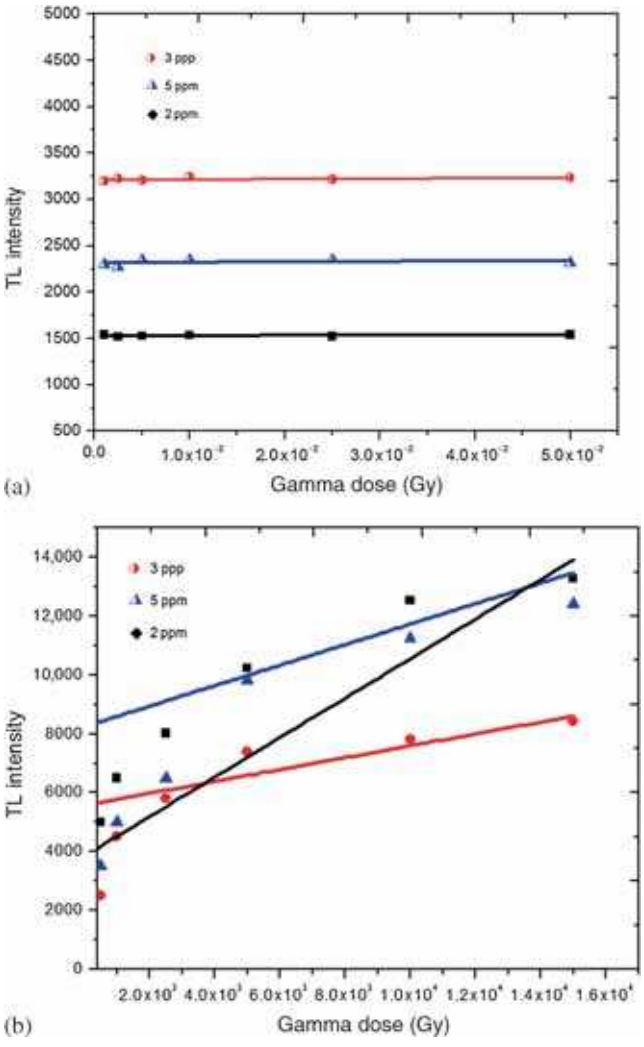

Figure 8. TL response of 50 mol% of Li_2O ($50B_2O_3$–$50Li_2O$) with 2, 3 and 5 ppm of Cu^{2+} (**a**) at low doses and (**b**) at high doses.

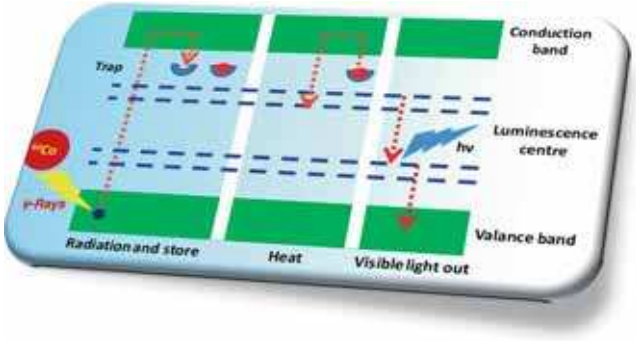

Figure 9. Representation of thermoluminescent properties.

the new energy levels within the energy gap of crystal. Hence, the transitions among these levels produced new optical band gaps in the perfect crystal. Hence, the released charge carriers could not recombine directly with luminescent centres. The energy of luminescent centres is transferred non-radiatively through the host lattice to the activator Cu^{2+}, which on recombination gives characteristic emission [39].

The comparison of TL response of the synthesized glass with 50 mol% of Li_2O ($50B_2O_3$–$50Li_2O$) with 2, 3 and 5 ppm of Cu^{2+} at low doses and 225°C is shown in figure 8a. It was observed that these materials did not display remarkable TL properties for lower doses in the range of 1×10^{-3} to 5×10^{-2} Gy. The result revealed that the ($50B_2O_3$–$50Li_2O$) with 3 ppm of Cu^{2+} showed high TL response, but was not a linear pattern so this compounds could not be recommended for low dose measurements. When these samples doped with different concentrations of Cu^{2+} were exposed for higher doses in the range of 1×10^1 to 20×10^3 Gy (figure 8b), it was found that, ($50B_2O_3$–$50Li_2O$) with 3 ppm of Cu^{2+} showed high TL as well as a linear response in the range of 1×10^1 to 5×10^2 Gy and supralinearity from 5×10^2 to 20×10^3 Gy. Whereas, the other corresponding compounds have also shown linear pattern when exposed to a gamma dose from 1×10^3 to 20×10^3 Gy. Therefore, the synthesized ($50B_2O_3$–$50Li_2O$) with 3 ppm of Cu^{2+} could be used as a TL material within this range. The TL response was related to the defects formed in the compounds under gamma irradiation, a decrease in their number might be the reason for

its reduction. Therefore, the low gamma doses are unable to create enough defect states to produce TL. On the other hand after increasing the dose [39], the total energy density overcomes the surface barrier to produce more defects states and enhance the TL intensity as shown in figure 9.

4. Conclusions

Copper ions-doped nanocrystalline $(100-x)B_2O_3$–xLi_2O : Cu^{2+} was prepared by the combustion method. TL characteristics of the synthesized material were studied at different parameters. The synthesized glass $50B_2O_3$–$50Li_2O$: Cu^{2+} with 3 ppm of doped Cu^{2+} exhibited superior TL properties than other glasses prepared in the current study. Therefore, the synthesized lithium borate doped with 3 ppm Cu^{2+} might be used for high dose measurements of gamma radiations. TL glow curves were recorded at different heating rates 1, 2, 5, 10, 15 and 20°C s^{-1} at fixed dose 10×10^3 Gy, and the results revealed that the glow peak position shifted to higher temperature with heating rate and the heating rate 10°C s^{-1} exhibited superior TL response with highest glow peak, which is a very good for dosimetry purposes, ($50B_2O_3$–$50Li_2O$: Cu^{2+}) with 3 ppm of Cu^{2+} showed high TL as well as a linear response in the range of 1×10^1 to 5×10^2 Gy and supralinearity from 5×10^2 to 20×10^3 Gy. While, the other corresponding compounds have also shown linear pattern when exposed to a gamma dose from 1×10^3 to 20×10^3 Gy. Therefore, the synthesized ($50B_2O_3$–$50Li_2O$) with 3 ppm of Cu^{2+} could be used as a TL material within this range.

Acknowledgement

This project was funded by the National Plan for Science, Technology and Innovation (MAARIFAH), King Abdul Aziz City for Science and Technology, Kingdom of Saudi Arabia, Award number (NAN-1005-02).

References

[1] Chen R and McKeever S W S 1997 *Theory of thermoluminescence and related phenomena* (Singapore: World Scientific)

[2] Furetta C 2003 *Handbook of thermoluminescence* (Singapore: World Scientific Publishing)

[3] McKeever S W S 1985 *Thermoluminescence of solids* (Cambridge: Cambridge University Press) Vol 69

[4] Pode R B and Dhoble S J 1998 *J. Phys. D: Appl. Phys.* **31** 146

[5] Morton D C and Forsythe E W 2001 *Appl. Phys. Lett.* **78** 1400

[6] Daniels F, Boyd C A and Saunders D F 1953 *Science* **117** 343

[7] Cameron J R, Daniels F, Johnson N and Kenney G 1961 *Science* **134** 333

[8] Bos A J J 2001 *Nucl. Instrum. Methods: Phys. Res. B, Beam Interact. Mater. Atoms* **184** 3

[9] Mathur V K, Lewandowski A C, Guardala N A and Price J L 1999 *Radiat. Meas.* **30** 735

[10] Dhoble S J, Moharil S V and Rao T K G 2001 *J. Lumin.* **93** 43

[11] Sangeeta S C and Sabharwal 2003 *J. Lumin.* **104** 267

[12] Naranje S M and Moharil S V 1998 *Phys. Status Solidi: Appl. Res.* **165** 489

[13] Stacy J J, Edelstein N and Mclaughlin R D 1972 *J. Chem. Phys.* **51** 4980

[14] Grant R M and Cameron J R 1966 *J. Appl. Phys.* **37** 3791

[15] Fang X, Zhai T, Gautam U K, Li L, Wu L, Bando Y and Golberg D 2011 *Prog. Mater. Sci.* **56** 175

[16] Harish G S, Divya A, Kumar K S and Reddy P S 2013 *Res. J. Phys. Sci.* **1** 7

[17] Huy B T, Quang V X and Chau H T B 2008 *J. Lumin.* **128** 601

[18] Li J, Hao J Q, Li C Y, Zhang C X, Tang Q, Zhang Y L, Su Q and Wang S B 2005 *Radiat. Meas.* **39** 229

[19] Li J, Hao J Q, Zhang C X, Tang Q, Zhang Y L, Su Q and Wang S B 2004 *Nucl. Instrum. Methods B* **222** 577

[20] Manma J and Sharma S K 2004 *J. Mater. Sci.* **39** 6203

[21] Driscoll C M H, Fisher E S, Furetta C and Padovani R 1983 *Radiat. Prot. Dosim.* **6** 305

[22] Ogorodnikov I N, Isaenko L I, Kruzhalov A V and Porotnikov A V 2001 *Radiat. Meas.* **33** 577

[23] Puppalwar S P, Dhoble S J, Dhoble N S and Kumar A 2012 *Nucl. Instrum. Methods B* **274** 167

[24] Thanh N Q, Quang V X, Khoi N and Dien N D 2008 *J. Sci. Math.–Phys.* **24** 97

[25] Siegel I and Lorenc J A 1966 *J. Chem. Phys.* **45** 2315

[26] Bates T 1962 *Modern aspects of the vitreous state* (London, UK: Butterworths) Vol 2

[27] Jorgensen C K 1955 *Acta Chem. Scand.* **9** 1362

[28] Ardelean I, Cozar O, Filip S, Pop V and Cenan I 1996 *Solid State Commun.* **100** 609

[29] Ardelean I, Peteanu M, Filip S, Simon V and Györffy G 1997 *Solid State Commun.* **102** 341

[30] Ciorcas F, Mendiratta S K, Ardelean I and Valente M A 2001 *Eur. Phys. J. B—Condens. Matter Complex Systems* **20** 235

[31] Jamal M, Shareefuddin M and Chary M N 1996 *Bull. Electrochem.* **12** 686

[32] Shareefuddin M, Vanaja K, Rao P M, Jamal M and Chary M N 1998 *Phys. Chem. Glasses* **39** 184

[33] Abragam A and Bleany B 1970 *EPR of transition metal ions* (Oxford: Clarendon)

[34] Bleany B D, Bowers K D and Ingram D J E 1955 *Proc. R. Soc. A* **228** 147

[35] Bates T and Mackenzie J D 1962 Modern aspects of the vitreous state (London: Butterworth) 2nd ed

[36] Taoufik I, Haddad M, Nadiri A, Brochu R and Berger R 1999 *J. Phys. Chem. Solids* **60** 701

[37] Esref T, Mehmet A, Mehmetand G and Mahmut U 2004 *J. Coord. Chem.* **57** 583

[38] Kumar D N and Garg B S 2006 *Spectrochim. Acta Part A* **64** 141

[39] Lochab S P, Pandey A, Sahare P D, Chauhan R S, Salah N and Ranjan R 2007 *Phys. Status Solidi A* **204** 2416